

CausalEGM: a general causal inference framework by encoding generative modeling

Qiao Liu[†], Zhongren Chen[†], Wing Hung Wong^{*}

Department of Statistics, Stanford University

December 14, 2022

Abstract

Although understanding and characterizing causal effects have become essential in observational studies, it is challenging when the confounders are high-dimensional. In this article, we develop a general framework *CausalEGM* for estimating causal effects by encoding generative modeling, which can be applied in both binary and continuous treatment settings. Under the potential outcome framework with unconfoundedness, we establish a bidirectional transformation between the high-dimensional confounders space and a low-dimensional latent space where the density is known (e.g., multivariate normal distribution). Through this, CausalEGM simultaneously decouples the dependencies of confounders on both treatment and outcome and maps the confounders to the low-dimensional latent space. By conditioning on the low-dimensional latent features, CausalEGM can estimate the causal effect for each individual or the average causal effect within a population. Our theoretical analysis shows that the excess risk for CausalEGM can be bounded through empirical process theory. Under an assumption on encoder-decoder networks, the consistency of the estimate can be guaranteed. In a series of experiments, CausalEGM demonstrates superior performance over existing methods for both binary and continuous treatments. Specifically, we find CausalEGM to be substantially more powerful than competing methods in the presence of large sample sizes and high dimensional confounders. The software of CausalEGM is freely available at <https://github.com/SUwonglab/CausalEGM>.

Keywords: Causal effect; Generative model; Potential outcome; Empirical risk

^{*}Corresponding Author. [†]Authors contributed equally to this research.

1 Introduction

Given the observational data, drawing inferences about the causal effect of a treatment is crucial to many scientific and engineering problems and attracts immense interest in a wide variety of areas. For example, (1) Zhang et al. (2017) investigated the effect of a drug on health outcomes in personalized medicine; (2) Panizza and Presbitero (2014) evaluated the effectiveness of public policies from the governments; (3) Kohavi and Longbotham (2017) conducted A/B tests to select a better recommendation strategy by a commercial company. Historically, the small sample size of many datasets imposes an impediment to meaningfully exploring the treatment effect by traditional subgroup analysis. In the big data era, there has been an explosion of data accumulation. We, therefore, require more powerful tools for accurate estimates of causal effects from large-scale observational data.

People are more interested in learning causation than correlation in causal inference. The most effective way to learn the causality is to conduct a randomized controlled trial (RCT), in which subjects are randomly assigned to an experimental group receiving the treatment/intervention and a control group for comparison. Then the difference between the experimental and control group of the outcome measures the efficacy of treatment/intervention. RCT has become the golden standard in studying causal relationships, as randomization can potentially limit all sorts of bias. However, RCT is time-consuming, expensive, and problematic with generalisability (participants in RCT are not always representative of their demographic). In contrast, observational studies can provide valuable evidence and examine effects in “real world” settings, while RCT tends to evaluate intervention effects under ideal conditions among highly selected populations. Given the observational data, we know each individual’s treatment, outcome, and confounders. The mechanism of how treatment causally affects the outcome needs to be discovered. One goal of observational study is to

estimate the counterfactual outcomes. For example, "would this patient have different health status if he/she received a different therapy?". In real-world applications, treatments are typically not assigned at random due to the selection bias introduced by confounders, thus may make the treated population differ significantly from the general population. Accurate estimation of the causal effect involves dealing with confounders, which are variables that affect both treatment and outcome. Failing to adjust for confounding effect may lead to biased estimates and wrong conclusions.

Many frameworks have been proposed to solve the above problems. The potential outcome model in Rubin (1974), also known as the Neyman–Rubin causal model, is arguably the most widely used framework. It makes precise reasoning about causation and the underlying assumptions. To measure the causal effect of a treatment, we need to compare the factual and counterfactual outcomes of each individual. As it is impossible to observe the potential outcomes of the same individual under different treatment conditions, the inference task can be viewed as a "missing data" problem where the counterfactual outcome needs to be estimated. Once we solve the "missing data" problem at an individual or a population-average level, the corresponding individual causal effect or average causal effect can be estimated.

Classic methods of non-parametric estimation of causal effect under the potential outcome framework include re-weighting, matching, and stratification, see Guo and Fraser (2014) in detail. These methods often perform well when the dimension of confounders is low, but break down when the number of confounders increases. In recent years, the prosperity of machine learning has largely accelerated the development of causal inference algorithms. In this article, we explore the advances in machine learning, especially deep learning, for improving the performance in causal effect estimation. We propose deep

generative methods, specifically, generative adversarial networks (GANs) to learn the latent representation of high-dimensional confounders. The independence of treatment and confounding variables conditioning on the latent representation provides a new aspect to handle the high-dimensional confounders.

1.1 Related works

With high accuracy and theoretical guarantees, our work contributes to the literature on estimating causal effects using deep generative models. Most of the works in this field are under binary treatment settings. For example, re-weighting methods, such as IPW from Rosenbaum (1987), and Robins et al. (1994) assign appropriate weight to each unit to eliminate selection bias. Matching-based methods provide a solution to directly compare the outcomes between the treated and control group within the matched samples. A detailed review of matching methods can be found in Stuart (2010). Another type of popular method in causal inference is based on the decision tree. These tree-based methods use non-parametric classification or regression by learning decision rules inferred from data. See Athey and Imbens (2016), Hill (2011) and Wager and Athey (2018). Recently, neural networks have been applied to causal inference, which demonstrates compelling and promising results. See Shalit et al. (2017), Shi et al. (2019), and Louizos et al. (2017), Yoon et al. (2018). Most of these efforts are under the binary treatment setting and focus on representation learning where the covariates are projected to a latent space. The limitations of these efforts mainly come from the following three perspectives. First, the information loss during representation learning is not controlled by the existing neural network models. A potential bias or decline in performance will be introduced if latent features can not capture enough variations in the covariates. Second, the multi-head model architecture

used by most of the approaches restricts the generalization ability of the model when the treatment is not discrete. Third, the dependency of latent variables on the treatment and outcome can not be distinguished. Besides, theoretical analysis for most existing neural network models is insufficient.

As for methods that deal with continuous treatment, a lot of efforts are focused on developing the theory of generalized propensity score. See the doubly robust estimators Robins and Rotnitzky (2001), the tree-based method Hill (2011), Lee (2018), and Galagat (2016) for other regression-based models. There are also non-parametric methods that do not require the correct specification of the models that relate the treatment or outcome to the covariates. See Flores et al. (2007), Kennedy et al. (2017), Fong et al. (2018) and Colangelo and Lee (2020). However, most of the regression-based methods require the specification of the relationship between covariates and treatment or outcome. For example, Galagat (2016) only considers the case when the average dose-response function (ADRF) is quadratic. Fong et al. (2018) relies on the assumption that the treatment has a linear relationship with covariates. On the one hand, such a strong assumption hinders the wide application of these methods. On the other hand, many of these methods fail under the presence of high dimensional covariates and cannot scale to large-scale datasets.

To overcome the above limitations, we develop CausalEGM, a general framework for estimating the treatment effect using encoding generative modeling. The CausalEGM model mainly differs from existing neural network methods in the following aspects. 1) Instead of using the multi-head architecture for estimating the factual and counterfactual outcomes, CausalEGM uses a uniform outcome function, which could deal with both binary and continuous treatments. 2) CausalEGM imposes an encoding-generative scheme to decouple the dependency of covariates on treatment and outcome, while existing methods do not

distinguish the dependencies. 3) We provide theoretical guarantees for the risk-bound analysis and the consistency analysis for the proposed method. From a technical point of view, the main contribution of this article is the proposal of a new general framework for estimating the causal effect under different treatment settings.

2 Method

2.1 Problem Formulation

We are interested in the causal effect of a variable X on another variable Y . X is usually called the treatment (or exposure) variable. Y is called the response (or outcome) variable. We assume Y is real-valued and $X \in \mathcal{X}$ where \mathcal{X} is either a finite set or a bounded interval in \mathbb{R} . X and Y are related by an outcome equation $Y = f(X, V, \epsilon)$ where V represents an observed multi-dimensional covariate, ϵ represents the set of other (unobserved) variables that may affect X and Y . Conceptually, $(Y, X, V, \epsilon) = (Y, X, V, \epsilon)(\omega)$ is a random variable whose value depends on the sampling unit ω in an underlying sample space Ω . We observe $(Y, X, V)(S_i)$ where $\{S_i, i = 1, \dots, n\}$ is an i.i.d sample drawn from Ω . The outcome equation f is unknown or assumed to belong to a very general class of functions.

To investigate causal effects, we assume that for each sampling unit ω , there is a set of “potential outcomes” for $\{Y(x)(\omega) = f(x, V(\omega), \epsilon(\omega)), x \in \mathcal{X}\}$ that are potentially measurable. For each sampling unit ω , how the outcome will response to changing treatment is given by the function $Y(\cdot)(\omega) : \mathcal{X} \rightarrow \mathbb{R}$. Thus, these unit-specific response functions capture the causal relations of interest. Our goal in this paper is to estimate their population average.

$$\mu(x) = \mathbb{E}(Y(x)) = \mathbb{E}(f(x, V, \epsilon))$$

Where the function $\mu(x)$ is known as the average dosage response function (ADRF) if X is continuous.

Since we only observe the potential outcome selected by the treatment variable $X(\omega)$, i.e., $Y(\omega) = f(X(\omega), V(\omega), \epsilon(\omega))$, the random variable $Y(x)$ is not directly observable, and its expectation $\mu(x)$ is generally not identifiable from the joint distribution of the observed (Y, X, V) . Additional assumptions are needed for the identification of $\mu(x)$. Typically, an “unconfoundedness” condition is imposed, which requires that ϵ and X are independent conditional on V . In other words, once V is given, there should be no unobserved confounding variables that drive correlated changes in the exposure and the outcome.

Assumption 1. (*unconfoundedness*) *Conditional on V , the treatment, X , is independent of ϵ ,*

$$X \perp\!\!\!\perp \epsilon | V.$$

Lemma 2.1. *Under Assumption 1, the ADRF is identifiable via the equation.*

$$\mu(x) = \int \mathbb{E}(Y|X = x, V = v)p_V(v)dv \quad \text{where } p_V(\cdot) \text{ is the marginal density of the } V.$$

If V is a low dimensional variable, the lemma suggests that we can estimate $\mu(x)$ by the empirical expectation $\hat{\mathbb{E}}(t(x, V))$ where $t(x, V)$ is an estimate of $\mathbb{E}(Y|X = x, V = v)$ obtained by nonparametric regression of Y on X and V . However, to ensure unconfoundedness, V should include all confounding covariates that can potentially affect both X and Y . Thus, in many applications, we must deal with a high-dimensional covariate V . This makes the method unattractive as high dimensional nonparametric regression is difficult in general. Furthermore, unlike the variables in V , the exposure variable X is a key variable that should be given special consideration, which is not the case for most non-parametric regression methods. This inherent tension between the size of V and the feasibility of nonparametric regression makes it difficult to use Lemma 2.1 for estimating μ .

To deal with this tension, in this paper we assume a modified version of unconfoundedness:

Assumption 2. *There exists a low dimensional feature $Z_0 = Z_0(V)$, which can be extracted from the high dimensional covariate V so that ϵ and V are independent of X conditional on Z_0 .*

Under Assumption 2, we have

$$\mu(x) = \int \mathbb{E}(Y|X=x, Z_0=z_0)p_{Z_0}(z)dz \quad (1)$$

Since Z_0 is of low dimension, it is easy to use (1) provided we know Z_0 as a function of V . Thus, the causal inference problem is transformed into the problem of learning $Z_0(V)$ from the i.i.d. sample $(Y_i, X_i, V_i) = (Y, X, V)(S_i) : i = 1, 2, \dots, n$. To learn this function, we propose a deep learning approach, which we call “Encoding Generative Modeling”, that allows simultaneous learning of an encoder for the high dimensional V and a generative model for (Y, X, V) . By imposing a suitable constraint on the generative model, one can ensure that certain subsets of the features computed by the encoder can be used as the low dimensional feature Z_0 in the above condition.

2.2 An Encoding Generative Model for Causal Inference

Our model is described in Figure 1. To handle the high dimension of V , we embed V into a low-dimensional latent space using an encoder function $Z = E(V)$ and a decoder function $V = G(Z)$. Note that such bidirectional transformation is inspired by our previous work Roundtrip for density estimation Liu et al. (2021). In a standard auto-encoder, these functions are learned by minimizing the reconstruction error between $G(E(V))$ and V over the observed data for V . Here, however, we will also impose a “distribution-matching” objective in addition to the reconstruction error. Specifically, assuming a pre-specified

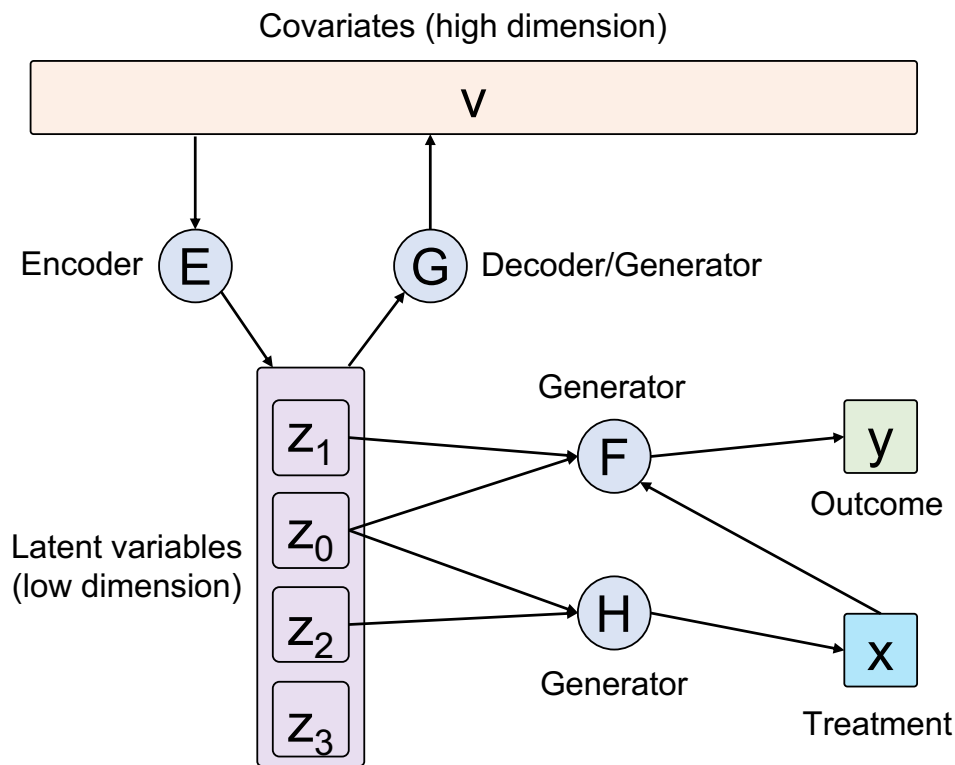


Figure 1: The overview of CausalEGM model. Variables are in rectangles. Functions are in circles, with incoming arrows indicating inputs to the function and outgoing arrows indicating outputs of the function. Each function is modeled by a neural network.

distribution for Z , we also want the distribution of $V^* = G(Z)$ to match the distribution of V . In this paper, the distribution for Z is assumed to be a standard Gaussian vector. Furthermore, there is a reconstruction objective for $E(G(Z))$ and a distribution matching objective for $E(V)$. We use deep neural networks to represent the functions $E()$ and $G()$. This part of our model, which deals with the relation between V and Z , can be viewed as an autoencoder for V where the decoder is required to serve as another generating function of a generative adversarial network (GAN). Following the common practice in the GAN literature, we use adversarial loss (i.e., maximizing the classification power between the generated and observed data) in addition to the reconstruction loss in the training. However, the learning of $E()$ and $G()$ should not be based on V alone. Rather, they must be coupled with the learning of generative models for X and Y , which are the variables of interest in our causal inference. To do this, we assume that the feature vector $Z = E(V)$ can be partitioned into different sub-vectors that have different roles in the generators for X and Y . Specifically, $Z = (Z_0, Z_1, Z_2, Z_3)$, $Y = F(X, Z_0, Z_1) + \epsilon_1$ and $X = H(Z_0, Z_2) + \epsilon_2$. These relations are depicted in the lower half of Figure 1, where for clarity, the independent noises ϵ_1 and ϵ_2 are not shown in the input to the generators. Conceptually, Z_0 represents the covariate features that affect both treatment and outcome, Z_1 represents the covariate features that affect only treatment, Z_2 represents the covariate features that affect only the outcome, and Z_3 represents the remaining covariate features that are also important for the representation of V . CausalEGM is highly flexible for handling different treatment settings. We just need to adjust the activation function in the last layer of the H network for different types of treatment.

2.3 Model training

The CausalEGM model consists of a bidirectional transformation module and two feed-forward neural networks. The bidirectional transformation module is used to project the covariates to a low-dimensional space and decouple the dependencies. This bidirectional module is composed of two generative adversarial networks (GANs). In one direction, the encoder network E aims to transform the covariates into latent features, whose distribution matches the standard multivariate Gaussian distribution. A discriminator D_z network tries to distinguish data sampled from the multivariate Gaussian distribution (labeled as positive one) from data generated by the E network (labeled as positive one). Similarly, there is another discriminator network in the GAN model that works in the reverse direction, where the generator/decoder network G transforms the latent feature back to the original covariate space to match the empirical distribution for the covariate. A discriminator network can be considered as a binary classifier where an input data point is classified to be either a positive one or a negative one. We use WGAN-GP Gulrajani et al. (2017) as the architecture for the GAN implementation, where the gradient penalty of discriminators is considered as an additional loss term. Thus, the loss function of the adversarial training for distribution matching in latent space has two terms

$$\begin{cases} \mathcal{L}_{GAN}(E) = - \mathbb{E}_{v \sim p_{emp}(v)} [D_z(E(v))] \\ \mathcal{L}_{GAN}(D_z) = - \mathbb{E}_{z \sim p(z)} [D_z(z)] + \mathbb{E}_{v \sim p_{emp}(v)} [D_z(E(v))] + \lambda \mathbb{E}_{z \sim \hat{p}(z)} [(\nabla D_z(z) - 1)^2] \end{cases} \quad (2)$$

where $p(z)$ and $p_{emp}(v)$ denote the multivariate Gaussian distribution and the empirical distribution of $\{\mathbf{v}_i\}_{i=1}^n$. $\hat{p}(z)$ and $\hat{p}(v)$ denoted the uniform sampling from the straight lines between the points sampled from observational data and generated data. Minimizing the loss of a generator (e.g., $L_{GAN}(E)$) and the corresponding discriminator (e.g., $L_{GAN}(D_z)$)

are adversarial as the two networks, E and D_z , compete with each other during the training process. λ is a penalty coefficient that is set to 10 in all experiments. The adversarial training of G and D_v is similar.

In addition to the GAN-based adversarial training losses, we introduced reconstruction losses to ensure that the reconstructed data is closed to the real data. The losses are represented as

$$\mathcal{L}_{rec}(E, G) = \|z - E(G(z))\|_2^2 + \|v - G(E(v))\|_2^2$$

Finally, to learn the generative models for the treatment and outcome variables, we impose the following mean squared error losses:

$$\begin{cases} \mathcal{L}_{MSE}(F) = \|x - F(z_0, z_2)\|_2^2 \\ \mathcal{L}_{MSE}(H) = \|y - H(z_0, z_1, x)\|_2^2 \end{cases} \quad (3)$$

We summarize all the loss functions above and group them by discriminator networks $\mathcal{L}(D_z, D_v)$ and other networks $\mathcal{L}(G, E, F, H)$:

$$\begin{cases} \mathcal{L}(G, E, F, H) = \mathcal{L}_{GAN}(E) + \mathcal{L}_{GAN}(G) + \mathcal{L}_{rec}(E, G) + \mathcal{L}_{MSE}(F) + \mathcal{L}_{MSE}(H) \\ \mathcal{L}(D_z, D_v) = \mathcal{L}_{GAN}(D_z) + \mathcal{L}_{GAN}(D_v) \end{cases} \quad (4)$$

We alternatively update the parameters in one of (E, G, F, H) or (D_z, D_v) given the value of the other.

2.4 Model architecture

The architecture of CausalEGM is highly flexible. In this work, we use fully-connected layers for all networks. Specifically, the (E, G, F, H) networks contain 5 fully-connected layers, and each layer has 64 hidden nodes. The (D_z, D_v) networks each contain 3 fully-connected layers, and each layer has 32 hidden nodes. The leaky-ReLu activation function is deployed

as a non-linear transformation in each hidden layer. We use Sigmoid as the activation function in the last layer of H network under the binary treatment setting. For continuous treatments, we do not use any activation function. Note that the Batch normalization is applied after each fully-connected layer. We use Adam optimizer with initial learning rate as 2×10^{-4} . The model parameters were updated in a mini-batch manner with the batch size equaling to 32.

3 Theoretical Analysis

We introduce a theoretical framework for analyzing GAN in Section 3.1. We then present the set up of our model in Section 3.2. Finally, we discuss the excess risk bound, generalization gap and consistency based on a few assumptions in Section 3.3 and 3.4.

3.1 GAN Background

Let P and Q be two probability measures on \mathbb{R} and \mathcal{A} be a class of measurable subsets of the input space \mathcal{X} . Then define $d(P, Q; \mathcal{A}) := \sup_{A \in \mathcal{A}} |P(A) - Q(A)|$. (Note if we let \mathcal{B} be the Borel sets, $d(P, Q; \mathcal{B})$ would become the variation distance between P and Q . Suppose P and Q have densities p and q , we then have $d(P, Q; \mathcal{B}) = \frac{1}{2} \|p - q\|_{L_1} = \frac{1}{2} \int |p - q|(x) d\mu(x)$.)

Let $\mathcal{A}_M := \{A \in \mathcal{A} : \exists D \in \mathcal{D}_M \text{ s.t. for all } x \in A, D(x) = 1\}$ where $D : \mathcal{X} \rightarrow \{0, 1\}$ indicates a classifier and \mathcal{D}_M is the set of classifiers constructed by deep neural networks with complexity parameter M (M can represent the number of layers, numbers of hidden nodes, etc.). Let $P_{emp} = \frac{1}{n} \sum_{i=1}^n \delta_{x_i}(x)$ where $\{x_i : i = 1, \dots, n\}$ is the set of observed samples. To train a classifier that distinguishes Q and P_{emp} , we find A^* s.t. $A^* = \arg \sup_{A \in \mathcal{A}_M} \|Q - P_{emp}\|_{L_1}$. WLOG, suppose $Q(A^*) - P_{emp}(A^*) > 0$, then $\forall A \in \mathcal{A}_M$, $Q(A^*) - P_{emp}(A^*) \geq Q(A) - P_{emp}(A)$. Now suppose $A = I_{\{D=1\}}$ for some classifier D , the

optimal discriminator D^* between Q and P_{emp} would give

$$Q(\{D^*(X) = 1\}) - P_{emp}(\{D^*(X) = 1\}) \geq Q(\{D(X) = 1\}) - P_{emp}(\{D(X) = 1\})$$

for all D in the class of discriminator under consideration. Thus, if Q_G is the probability distribution for $G(Z)$, the adversarial training is then equivalent to solving the minimization problem

$$\inf_G \sup_{A \in \mathcal{A}} |Q_G(A) - P_{emp}(A)| = \inf_G d(Q_G, P_{emp}; \mathcal{A}_M)$$

3.2 Problem Setup and Notation

Now for the CausalEGM, suppose

$$\left\{ \begin{array}{l} Y = f^0(X, Z_0, Z_1) + \epsilon_1, \\ X = h^0(Z_0, Z_2) + \epsilon_2, \\ (Z_0, Z_1, Z_2) = (e_0^0(v), e_1^0(v), e_2^0(v)), \\ \mathbb{E}[\epsilon_1] = \mathbb{E}[\epsilon_2] = 0, \quad var(\epsilon_1) = \sigma_1, \quad var(\epsilon_2) = \sigma_2. \end{array} \right. \quad (5)$$

where f^0 , h^0 , e^0 , and g^0 are the unknown underlying functions that relate Y , X , V , and Z . We aim to train f , h , e , and g using CausalEGM to approximate f^0 , h^0 , e^0 , and g^0 . We want the latent variable $Z = (Z_0, Z_1, Z_2, Z_3)$ to have a fixed distribution (e.g., multivariate Gaussian) so that both f and h are generative models and e to be a good encoder that will capture most of the variation in V . Let $V \in \mathcal{V}$ be a continuous random variable in a p -dimensional space. We aim to learn two mappings $e : \mathcal{V} \rightarrow \mathbb{R}^q$ and $g : \mathbb{R}^q \rightarrow \mathcal{V}$ where $p \ll q$. Denote Z^0 as the random variable that follows a standard multivariate Gaussian distribution. Then we want our trained encoder e to satisfy:

$$e(V) \sim Z^0 \quad (6)$$

In order for g to reconstruct $e(V)$, $e(\cdot)$ and $g(\cdot)$ should minimize $\mathbb{E}_0\|V - g(e(V))\|_2^2$.

Accordingly, we design the loss functions:

$$\begin{cases} L_1 = \mathbb{E}_n\|Y - f(X, e_0(V), e_1(V))\|_2^2 \\ L_2 = \mathbb{E}_n\|X - h(e_0(V), e_2(V))\|_2^2 \\ L_3 = \sup_{A \in \mathcal{A}_m} |P(A; Z^0) - P_{emp}(A; e(V))| = d(P_{Z^0}, P_{emp(e(V))}; \mathcal{A}_m) \\ L_4 = \mathbb{E}_n\|V - g(e(V))\|_2^2 \end{cases} \quad (7)$$

where \mathbb{E}_n is the empirical expectation. P_{Z^0} is the probability measures of Z^0 and $P_{emp(e(V))}$ is the empirical distribution of $e(V)$. The empirical risk is denoted as follows:

$$R_{emp} = L_1 + L_2 + L_3 + L_4$$

Hence the corresponding true risk is:

$$R^0 = R_1^0 + R_2^0 + R_3^0 + R_4^0$$

where

$$\begin{cases} R_1^0 = \mathbb{E}_0\|Y - f(X, Z_0, Z_1)\|_2^2 \\ R_2^0 = \mathbb{E}_0\|X - h(Z_0, Z_2)\|_2^2 \\ R_3^0 = d(P_{Z^0}, P_{e(V)}; \mathcal{A}_m) \\ R_4^0 = \mathbb{E}_0\|V - g(e(V))\|_2^2 \end{cases} \quad (8)$$

where \mathbb{E}_0 stands for the expectation w.r.t the underlying distribution of the random variables and $P_{e(V)}$ is the probability measure induced by $e(V)$. Denote \mathcal{F}_M as the class of deep neural networks of complexity M . Let $\hat{f}_M, \hat{h}_M, \hat{e}_M$ and \hat{g}_M to be the solution of $\inf_{f, h, e, g \in \mathcal{F}_M} R_{emp}(f, h, e, g)$ and f_M^0, h_M^0, e_M^0 and g_M^0 be the solution of $\inf_{f, h, e, g \in \mathcal{F}_M} R^0(f, h, e, g)$. So $(\hat{f}_M, \hat{h}_M, \hat{e}_M, \hat{g}_M)$ is the solution of minimizing empirical risk and $(f_M^0, h_M^0, e_M^0, g_M^0)$ is the solution of minimizing the true risk.

3.3 Excess risk bound

We can now define the excess risk within the class \mathcal{F}_M :

$$R^0(\hat{f}_M, \hat{h}_M, \hat{e}_M, \hat{g}_M) - \inf_{f, h, e, g \in \mathcal{F}_M} R^0(f, h, e, g) = R^0(\hat{f}_M, \hat{h}_M, \hat{e}_M, \hat{g}_M) - R^0(f_M^0, h_M^0, e_M^0, g_M^0)$$

Before moving forward, we first make some assumptions on the \mathcal{F}_M .

Assumption 3. (*b-uniformly bounded*) $\bigcup_M \mathcal{F}_M$ is *b-uniformly bounded*: there exists some $b > 0$ such that for any $f \in \bigcup_M \mathcal{F}_M$, $\|f\|_\infty \leq b$.

Assumption 4. (*uniformly equi-continuous*) $\bigcup_M \mathcal{F}_M$ is *uniformly equi-continuous*: $\forall \epsilon > 0$, there exists a $\delta > 0$ such that for any $f_1, f_2 \in \bigcup_M \mathcal{F}_M$,

$$|f_1(x) - f_2(y)| < \epsilon$$

whenever $|x - y| < \delta$.

Note the above assumptions can be ensured by putting constraints on the gradients of functions and bounding the domain of the input space. We are now able to show that the excess risk converges to zero in probability as $M, n \rightarrow \infty$ where M denotes the complexity of the class of neural networks and n denotes the number of sample points. Denote $P_{Z_{emp}}$ as the empirical distribution of Z .

Lemma 3.1.

$$R^0(\hat{f}_M, \hat{h}_M, \hat{e}_M, \hat{g}_M) \leq \inf_{f, h, e, g \in \mathcal{F}_M} R^0(f, h, e, g) + \alpha_{M,n} + \beta_{M,n} + \gamma_{M,n} + \zeta_{M,n}$$

where

$$\left\{ \begin{array}{l} \alpha_{M,n} = 2 \sup_{f \in \mathcal{F}_M} |(\mathbb{E}_n - \mathbb{E}_0)(\|Y - f(X, Z_0, Z_1)\|_2^2)| \\ \beta_{M,n} = 2 \sup_{h \in \mathcal{F}_M} |(\mathbb{E}_n - \mathbb{E}_0)(\|X - h(Z_0, Z_2)\|_2^2)| \\ \gamma_{M,n} = 2d(P_{Z_{emp}}, P_{Z^0}; \mathcal{A}_M) \\ \zeta_{M,n} = 2 \sup_{g, e \in \mathcal{F}_M} |(\mathbb{E}_n - \mathbb{E}_0)(\|V - g(e(V))\|_2^2)| \end{array} \right. \quad (9)$$

Theorem 3.2. (Bound of Excess Risk) Denote $O := (Y, X, Z_0, Z_1, Z_2)$. Then we define the Rademacher complexity of a function class \mathcal{F} as $\mathcal{R}_n(\mathcal{F}) := \mathbb{E}_{\epsilon, O}[\sup_{f \in \mathcal{F}} |\frac{1}{n} \sum_{i=1}^n \epsilon_i f(O_i)|]$ where $\epsilon_1, \epsilon_2, \dots, \epsilon_n$ are independent random variables drawn from the Rademacher distribution. For any $\delta > 0$, we have

$$R^0(\hat{f}_M, \hat{h}_M, \hat{e}_M, \hat{g}_M) - \inf_{f, h, e, g \in \mathcal{F}_M} R^0(f, h, e, g) \leq 16\mathcal{R}_n(\mathcal{F}_M) + \delta$$

with probability at least $1 - 16e^{-\frac{n\delta^2}{2b^2}}$.

We can also look at the generalization gap, which is the difference between the empirical risk and the expected risk. It measures how accurately the model is to predict values for unseen data. In our context, given a quadruple of functions (f, h, e, g) , the generalization gap is defined to be:

$$R_{emp}(f, h, e, g) - R^0(f, h, e, g)$$

Theorem 3.3 (Generalization Gap). Given a quadruple of functions $(f, h, e, g) \in \mathcal{F}_M$, for any $\delta > 0$, we have

$$R_{emp}(f, h, e, g) - R^0(f, h, e, g) \leq 4\mathcal{R}_M(\mathcal{F}_M) + \delta$$

for any $\delta > 0$ with probability at least $1 - 4e^{-\frac{n\delta^2}{2b^2}}$.

3.4 Consistency analysis

With one more assumption, we can then show the consistency of our neural networks.

Assumption 5. *There exists \tilde{e}_3 , \tilde{g} and $\delta > 0$ s.t.*

$$(e_0^0, e_1^0, e_2^0, \tilde{e}_3) \stackrel{\mathcal{D}}{=} Z^0 \quad (10)$$

where the quadruplet denotes the four component of the encoder function and for any function e and g ,

$$\mathbb{E}_0 \|V - \tilde{g}((e_0^0, e_1^0, e_2^0, \tilde{e}_3)(V))\|_2^2 \leq \mathbb{E}_0 \|V - g((e)(V))\|_2^2 + \delta \quad (11)$$

We provided a concrete simulation example in appendix B to verify the rationality of the Assumption 5.

From Assumption 3 and Assumption 4 we conclude that $\bigcup_M \mathcal{F}_M$ is sequentially compact by Arzelà–Ascoli theorem. Hence $\bigcup_M \mathcal{F}_M$ is a *Glivenko-Cantelli* class and $\mathcal{R}_n(\bigcup_M \mathcal{F}_M) \rightarrow 0$ as $n \rightarrow \infty$. Now let $m : \mathbb{N} \rightarrow \mathbb{N}$ be a strictly increasing function s.t. $\lim_{n \rightarrow \infty} \mathcal{R}_n(\mathcal{F}_{m_n}) = 0$. Let $(\hat{f}, \hat{h}, \hat{e}, \hat{d})_n$ be the sequence of quadruple that solves $\inf_{f, h, e, d \in \mathcal{F}_{m_n}} R_{emp}$, then there exists a limit point of this sequence as $n \rightarrow \infty$.

Theorem 3.4. (*Consistency*)

Let (f^*, h^*, e^*, g^*) be any limit point of $(\hat{f}, \hat{h}, \hat{e}, \hat{g})_n$. We then have

$$\mathbb{E}_0 \|(f^0 - f^*)(X, Z_0, Z_1)\|_2^2 + \mathbb{E}_0 \|(h^0 - h^*)(Z_0, Z_2)\|_2^2 + d(P_{Z^0}, P_{e^*(V)}; \mathcal{A}_M) \leq 2\delta$$

for some small $\delta > 0$.

Theorem 3.4 suggests that if V can be encoded effectively s.t. the Assumption 5 are satisfied with $\delta \approx 0$, we would have approximately

$$f^* \approx f^0, h^* \approx h^0, e^*(V) \stackrel{\mathcal{D}}{\approx} Z^0.$$

This holds for any limit points of $\{(\hat{f}, \hat{h}, \hat{e}, \hat{g})_n\}$.

4 Experiments

To demonstrate the power of CausalEGM, we designed a series of experiments to evaluate the performance of CausalEGM against some state-of-the-art methods. In observational studies, accurately estimating the treatment effects on the population level and individual level are both crucial. We aim to verify the ability of CausalEGM to estimate both the average treatment effect on the population level and the individual treatment estimation concerning the heterogeneous treatment effects. Since CausalEGM is applicable for both binary treatment and continuous treatment, we test the performance of CausalEGM under both settings.

4.1 Datasets

For the continuous treatment setting, three simulation datasets and one real dataset used in existing studies were introduced.

Hirano and Imbens We use a similar data-generating process as in Hirano and Imbens (2004) and Moodie and Stephens (2012) as follows: let V_1, V_2, \dots, V_p be unit exponential, $Z_0 = V_1$, $Z_1 = V_2$, $Z_2 = V_3$, $X|V \sim \exp(Z_0 + Z_1)$, $Y(x)|V \sim N(x + (Z_0 + Z_2)\exp(-x(Z_0 + Z_2)), 1)$. Then the dose response function can be obtained by integration w.r.t the covariates V :

$$\mu(x) = x + \frac{2}{(1+x)^3}$$

Sun We generate a synthetic dataset using a similar data generating process described in Sun et al. (2015). with some modifications to fit for continuous treatment. Specifically, we let $V_1, \dots, V_p \stackrel{iid}{\sim} N(0, 1)$ and define $f_1(u) = -2\sin(2u)$, $f_2(u) = u^2 - \frac{1}{3}$, $f_3(u) = u - \frac{1}{2}$, $f_4(u) = \cos(u)$, $f_5(u) = u^2$ and $f_6(u) = u$. We then generate the treatment to be $X \sim N(\sum_{i=1}^4 f_i(V_i), 1)$ and the outcome to be $Y \sim N(X + f_3(V_1) + f_4(V_2) + f_5(V_5) + f_6(V_6), 1)$.

Then the dose response function can be obtained by integration w.r.t the covariates V :

$$\mu(x) = x + 0.5 + e^{-0.5}.$$

Colangelo and Lee We followed a similar data generation process in Colangelo and Lee (2020) as follows: let $\epsilon_1 \sim N(0, 1)$, $\epsilon_2 \sim N(0, 1)$. The covariates are generated by $V = (V_1, \dots, V_{100})' \sim N(0, \Sigma)$ where $diag(\Sigma) = 1$ and $\Sigma_{i,j} = 0.5$ for $|i-j| = 1$. The treatment is generated by $X = \Phi(3V'\theta) + 0.75\epsilon_1 - 0.5$ where $\theta_j = 1/j^2$. The outcome is generated by $Y = 1.2X + 1.2V'\theta + X^3 + XV_1 + \epsilon_2$. The dose response function is $\mu(x) = 1.2x + x^3$.

Twins This contains data of 71,345 twins, including their weights (used as treatment), mortality, and 50 other covariates (so $p = 50$) derived from all births in the USA between 1989-1991. Similar to Li et al. (2020), we first filtered the data by limiting the weight to be less than 2 kilograms. 4821 pairs of twins were kept for further analysis. We then set the weights as the continuous treatment variable. We can then semi-simulate the risk of death (outcome) based on the observation that higher weight leads to lower death rate in general, which we formulated as $Y = -\frac{2}{1+e^{-3x}} + v\gamma + \epsilon$ where $\gamma \in \mathbb{R}^{p \times 1}$ and $\gamma_i \sim N(0, 0.025^2)$, $\epsilon \sim N(0, 0.25^2)$. The ADRF is then: $\mu(x) = -\frac{2}{1+e^{-3x}} + \mathbb{E}[V_i \cdot \gamma]$.

For binary treatment setting, we introduced the IBM dataset, which is the most comprehensive benchmark dataset in this field. The IBM dataset is semi-synthetic and derived from the linked birth and infant death data (LBIDD). 117 measured covariates are given, while the treatment and outcome are simulated based on 63 different data-generating processes. The sample size varies from 1,000 to 50,000.

4.2 Evaluation metrics

In the continuous treatment setting, we aim to evaluate whether the estimated dose-response function $\mu(x)$ can well approximate the true dose-response function. Three different metrics are used.

Root-Mean-Square Error (RMSE)

$$RMSE = \sqrt{\frac{1}{N} \sum_{i=1}^N \|\mu(x_i) - \hat{\mu}(x_i)\|_2^2} \quad (12)$$

Mean Absolute Percentage Error (MAPE)

$$MAPE = \frac{1}{N} \sum_{i=1}^N \left\| \frac{\mu(x_i) - \hat{\mu}(x_i)}{\mu(x_i)} \right\|_1 \quad (13)$$

Mean Absolute Error of MTFE (Bias(MTFE)) We first calculate *Marginal Treatment Effect Function* (MTFE) at x as:

$$MTEF = \frac{\mu(x + \Delta x) - \mu(x)}{\Delta x} \quad (14)$$

Then Mean Absolute Error of MTFE (Bias(MTFE)) is then defined to be the mean absolute difference between the ground truth MTFE using $\mu(x)$ and the estimated MTFE using $\hat{\mu}(x)$.

In binary treatment settings, we consider both the population-level average treatment effect and individual treatment effect. Two commonly used metrics are introduced as follows.

Absolute Error in Average Treatment Effect (ϵ_{ATE})

$$\epsilon_{ATE} = \left| \frac{1}{n} \sum_{i=1}^n (\hat{Y}_i(1) - \hat{Y}_i(0)) - \frac{1}{n} \sum_{i=1}^n (Y_i(1) - Y_i(0)) \right|$$

Precision in Estimation of Heterogeneous Effect (ϵ_{PEHE})

$$\epsilon_{PEHE} = \frac{1}{n} \sum_{i=1}^n (\hat{Y}_i(1) - \hat{Y}_i(0) - (Y_i(1) - Y_i(0)))^2$$

4.3 Baselines

For continuous treatment setting, three different baselines were used.

Ordinary Least Squares regression (OLS). OLS first fit a linear regression model for $Y|(X, V)$. For each value of treatment x , the estimated ADRF is then $\frac{1}{n} \sum_i^n ls(x, v_i)$ where ls is the fitted linear model.

Regression Prediction Estimator (REG). See Schafer and Galagate (2015), Galagate (2016), and Imai and Van Dyk (2004). This method generalizes the notion of *prima facie* estimator. It takes the covariates into account when doing regression.

Double Debiased Machine Learning Estimator (DML). See Colangelo and Lee (2020). DML is a kernel-based machine learning approach that combines a doubly moment function and cross-fitting. Various machine learning methods can be used to estimate the conditional expectation function and conditional density. We used "Lasso" and "Neural network" provided by the DML as two variants, denoted as DML(lasso) and DML(nn).

For binary treatment setting, four baselines were introduced.

CFR. CFR Shalit et al. (2017) estimated the individual treatment effect (ITE) by utilizing neural networks to learn the low-dimensional representation for covariates and two outcome functions, respectively. An integral probability metric was further introduced to control the balance of distributions in the treated and control group. We use the two variants of CFR for comparison, which are referred to as TAENET and CFRNET.

Dragonnet. Dragonnet Shi et al. (2019) used a three-head architecture, which contains a two-head architecture for outcome estimation and a one-head architecture for propensity

score estimation. It is noted that Dragonnet uses essentially the same architecture as CFR if the propensity-score head is removed.

CEVAE. CEVAE Louizos et al. (2017) is a variational autoencoder-based method for estimating the treatment effect where a TARnet architecture was used in the inference network and the latent variables were set to be multivariate normal distribution.

GANITE. GANITE =Yoon et al. (2018) exploited a generative adversarial network (GAN) model for generating the counterfactual outcome through adversarial training.

4.4 Results

We first evaluate the performance of CausalEGM model in the continuous setting where the treatment $x \in \mathcal{X}$ and \mathcal{X} is a bounded interval in \mathbb{R} . We compared CausalEGM with four different methods, including one using neural networks as its key component. It is shown that CausalEGM demonstrates superior results over the existing methods, including two linear regression-based methods OLS and REG, and a kernel-based machine learning approach with two different machine learning algorithms (lasso and neural network). We first evaluate whether the dose-response function can be well estimated by different competing methods. It is observed that OLS and Reg result in relatively large estimation errors. The dose-response curves estimated by the DML methods possess spikes and fluctuation. In contrast, the curves estimated by CausalEGM are smooth and the estimates are of small errors.

In terms of the quantitative measurements, CausalEGM achieves the lowest RMSE, MAPE, Bias(MTEF) in all three simulation datasets compared to baseline methods (Table 1). We also note that DML method performs much better than linear regression-based methods (OLS and REG) in Hiranos and Imbens and Twins datasets while performing less

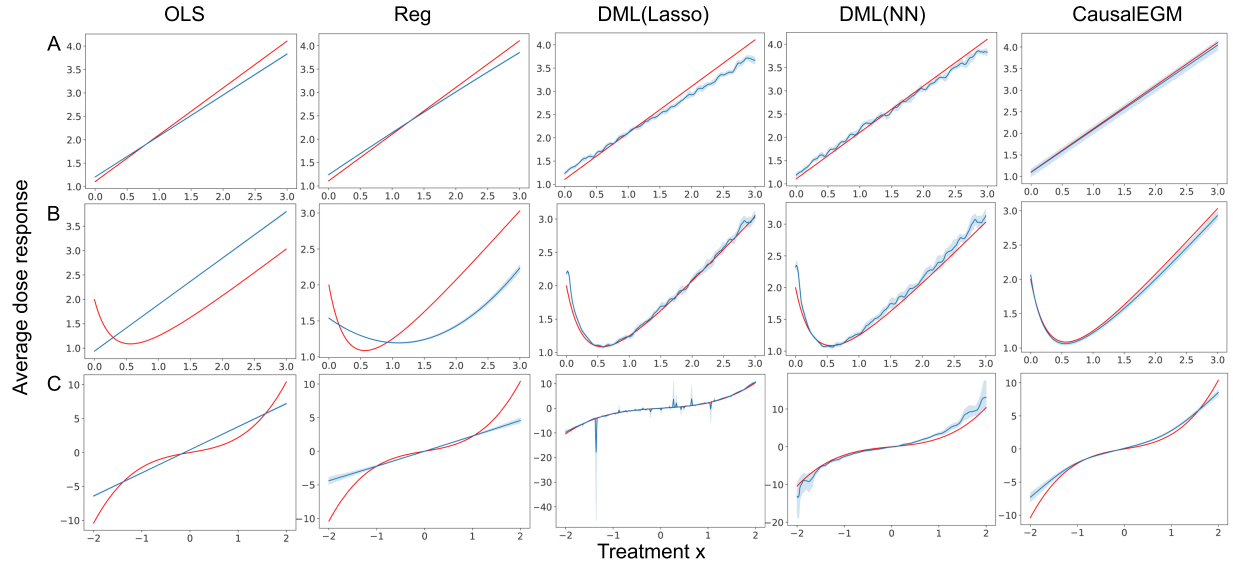


Figure 2: The performance of CausalEGM and baseline methods (OLS, Reg, DML with Lasso or neural network) under continuous treatment settings across three benchmark datasets. (A) Hiranos and Imbens dataset. (B) Sun et al dataset. (C) Colangelo and Lee dataset. The red curves are the ground truth while the blue curves are the estimated average dose response with 95% confidence interval based on 10 independent simulations.

Dataset	Method	RMSE	MAPE	Bias(MTEF)
Hiranos and Imbens	OLS	0.673 ± 0.0126	0.364 ± 0.00501	0.628 ± 0.00862
	REG	0.512 ± 0.0311	0.210 ± 0.00956	0.577 ± 0.025
	DML(lasso)	0.0932 ± 0.0113	0.0378 ± 0.00501	1.63 ± 0.190
	DML(nn)	0.152 ± 0.0282	0.0615 ± 0.0126	501 ± 386
	CausalEGM	0.0706 ± 0.0445	0.0352 ± 0.0210	0.0889 ± 0.0210
Sun et al	OLS	0.141 ± 0.0151	0.0412 ± 0.00312	0.125 ± 0.00729
	REG	0.119 ± 0.0102	0.0402 ± 0.00265	0.128 ± 0.00757
	DML(lasso)	0.188 ± 0.0263	0.0576 ± 0.00504	1.64 ± 0.106
	DML(nn)	1.75 ± 0.0125	5.11 ± 0.0849	555 ± 318
	CausalEGM	0.0436 ± 0.0085	0.0180 ± 0.0038	0.0230 ± 0.0116
Colangelo and Lee	OLS	1.32 ± 0.025	1.27 ± 0.114	2.02 ± 0.00469
	Reg	2.05 ± 0.133	0.484 ± 0.0498	2.17 ± 0.0446
	DML(Lasso)	1.92 ± 2.80	0.830 ± 0.852	1860 ± 3906
	DML(nn)	1.95 ± 1.27	0.737 ± 0.193	5919 ± 5297
	CausalEGM	0.886 ± 0.232	0.426 ± 0.124	1.66 ± 0.290
Twins	OLS	0.106 ± 0.002	4.0 ± 12.0	0.320 ± 0.0002
	Reg	9.77 ± 6.07	87.9 ± 212.0	7.19 ± 5.82
	DML(Lasso)	0.0815 ± 0.0144	1.91 ± 5.37	6.06 ± 1.61
	DML(nn)	0.100 ± 0.040	2.92 ± 8.28	190 ± 311
	CausalEGM	0.0242 ± 0.0132	0.499 ± 1.39	0.0746 ± 0.0314

Table 1: Result on synthetic datasets with sample size $n = 20000$, number of covariates $p = 200$. Standard deviations of metrics of 10 times experiments are indicated by the values in brackets.

well in the other two. CausalEGM reduces the RMSE, MAPE, Bias(MTEF) by 24.2% to 63.4%, 6.9% to 55.2%, and 17.8% to 84.6% compared to the best baseline method across different datasets, respectively. The results of both simulation data and real data illustrate that CausalEGM is powerful for estimating the causal effect in continuous settings.

In binary treatment settings where the treatment $x \in \{0, 1\}$, we aim to evaluate whether CausalEGM could estimate an accurate treatment effect. CausalEGM was benchmarked against a series of state-of-the-art methods on the IBM benchmark datasets, which provide various simulation settings and sample sizes. We chose three datasets from each of three

Metric	Dataset	TARNET	CFRNET	CEVAE	GANITE	Dragonnet	CausalEGM
ϵ_{ATE}	Datasets-1k	0.022 \pm 0.015	0.035 \pm 0.013	0.035 \pm 0.021	0.27 \pm 0.08	0.010 \pm 0.004	0.023 \pm 0.016
		0.038 \pm 0.029	0.022 \pm 0.014	0.11 \pm 0.10	1.97 \pm 0.30	0.012 \pm 0.007	0.066 \pm 0.020
		3.05 \pm 0.01	3.04 \pm 0.002	0.16 \pm 0.12	6.42 \pm 0.84	0.32 \pm 0.14	0.154 \pm 0.057
	Datasets-10k	6.44 \pm 3.49	12.00 \pm 7.03	204 \pm 58	2.67 \pm 1.23	124 \pm 11	3.52 \pm 0.48
		0.055 \pm 0.001	0.060 \pm 0.001	0.070 \pm 0.031	1.22 \pm 0.17	0.0097 \pm 0.069	0.0039 \pm 0.0026
		0.034 \pm 0.023	0.0592 \pm 0.0015	0.018 \pm 0.011	0.12 \pm 0.09	0.078 \pm 0.057	0.0162 \pm 0.0150
	Datasets-50k	0.045 \pm 0.002	0.045 \pm 0.001	0.38 \pm 0.22	0.34 \pm 0.07	0.0089 \pm 0.0083	0.003 \pm 0.002
		0.044 \pm 0.003	0.045 \pm 0.004	0.66 \pm 0.59	2.26 \pm 0.15	0.027 \pm 0.028	0.0052 \pm 0.0045
		0.2950 \pm 0.0004	0.2950 \pm 0.002	0.64 \pm 0.45	1.86 \pm 0.29	0.16 \pm 0.08	0.0098 \pm 0.0061
ϵ_{PEHE}	Datasets-1k	0.11 \pm 0.02	0.0015 \pm 0.0009	0.012 \pm 0.005	0.14 \pm 0.04	0.038 \pm 0.003	0.053 \pm 0.006
		0.35 \pm 0.03	0.29 \pm 0.04	0.27 \pm 0.04	4.34 \pm 1.24	0.34 \pm 0.01	0.30 \pm 0.03
		18.30 \pm 0.29	18.90 \pm 0.26	0.15 \pm 0.10	42.9 \pm 10.0	0.32 \pm 0.13	0.14 \pm 0.04
	Datasets-10k	433 \pm 106	662 \pm 288	46200 \pm 15500	78.7 \pm 26.8	22200 \pm 4130	14.90 \pm 4.22
		0.024 \pm 0.005	0.022 \pm 0.006	0.091 \pm 0.019	2.08 \pm 0.45	0.042 \pm 0.003	0.020 \pm 0.001
		0.012 \pm 0.005	0.0040 \pm 0.0028	0.0034 \pm 0.0013	0.14 \pm 0.08	0.036 \pm 0.015	0.0040 \pm 0.012
	Datasets-50k	0.00098 \pm 0.00102	0.00133 \pm 0.00092	0.013 \pm 0.021	0.34 \pm 0.13	0.0059 \pm 0.0020	0.00018 \pm 0.00008
		0.88 \pm 0.04	0.904 \pm 0.084	1.12 \pm 0.50	3.64 \pm 1.40	1.012 \pm 0.056	0.80 \pm 0.03
		0.13 \pm 0.04	0.338 \pm 0.153	9.86 \pm 6.36	15.00 \pm 8.73	1.93 \pm 0.74	0.059 \pm 0.023

Table 2: The performance of CausalEGM and comparison methods in IBM benchmark datasets with various sample sizes. Each method was run 10 times and the standard deviations are shown. The best performance is marked in bold.

different sample sizes (1k, 10k, and 50k) with the most complicated generation process (e.g., the generation functions are of the highest order). CausalEGM was compared to five baseline methods on each of these datasets. As shown in Table 2, CausalEGM achieves the smallest ϵ_{ATE} in 6 out of 9 datasets and the smallest ϵ_{PEHE} in 7 out of 9 datasets. CausalEGM performs especially well in datasets with large sample sizes (e.g., 50k). For example, the ϵ_{ATE} and ϵ_{PEHE} are reduced by 66.3% to 93.9%, and 9.1% to 86.5% in the three largest datasets compared to the second best method, respectively. To sum up, our model shows superior performance in estimating both average treatment effect and individual treatment effect and is substantially more powerful than competing methods when the sample size is large.

Dataset	Method	RMSE	MAPE	Bias(MTEF)
Hiranos and Imbens	CausalEGM w/o RT	0.0936 ± 0.0579	0.0434 ± 0.0293	0.128 ± 0.0624
	CausalEGM	0.0706 ± 0.0445	0.0352 ± 0.0210	0.0889 ± 0.0210
Sun et al	CausalEGM w/o RT	0.106 ± 0.0473	0.0438 ± 0.0224	0.0305 ± 0.0147
	CausalEGM	0.0436 ± 0.0085	0.0180 ± 0.0038	0.0230 ± 0.0116
Colangelo and Lee	CausalEGM w/o RT	1.28 ± 0.129	0.488 ± 0.0950	2.21 ± 0.109
	CausalEGM	0.886 ± 0.232	0.426 ± 0.124	1.66 ± 0.290
Twins	CausalEGM w/o RT	0.0641 ± 0.0252	2.38 ± 6.64	0.0903 ± 0.0346
	CausalEGM	0.0242 ± 0.0132	0.499 ± 1.39	0.0746 ± 0.0314

Table 3: Ablation study on evaluating the contribution of Roundtrip module. Each method was run for 10 times and the standard deviations are shown.

We have demonstrated that the performances of CausalEGM under both continuous and binary treatment settings are superior. Since our model is composed of multiple neural networks, it is necessary to evaluate the contribution of different components. We first evaluated the contribution of the Roundtrip module. To do this, we removed the G network and the discriminator networks D_z and D_v and denoted the model as CausalEGM w/o RT, which no longer requires adversarial training and reconstruction for v and z . Taking the continuous treatment setting for an example, we note that the performance of CausalEGM without the Roundtrip module has a noticeable decline in all datasets. The RMSE, MAPE, Bias(MTEF) increases by 32.68% to 164.88%, 14.55% to 376.95%, and 21.85% to 43.98%, respectively (Table 3). Such experimental results imply that the adversarial training and the reconstruction error are essential for learning a good low-dimensional representation of the high-dimensional covariates.

Next, we investigate whether the adversarial training and the reconstruction error objectives are necessary in the Roundtrip module. In our model design, the adversarial training in latent space is necessary to guarantee the independence of latent variables. The reconstruction of V is also required for ensuring the latent features contain all the information

Dataset	(V-GAN, Z-Rec)	RMSE	MAPE	Bias(MTFE)
Hiranos and Imbens	(1,1)	0.0906 \pm 0.0270	0.0439 \pm 0.0116	0.104 \pm 0.200
	(0,1)	0.0727 \pm 0.0451	0.0345 \pm 0.0190	0.0890 \pm 0.0230
	(1,0)	0.0845 \pm 0.0321	0.0401 \pm 0.00984	0.0940 \pm 0.0355
	(0,0)	0.0784 \pm 0.0363	0.0371 \pm 0.0163	0.103 \pm 0.0352
Sun et al	(1,1)	0.0567 \pm 0.0299	0.0219 \pm 0.0134	0.0280 \pm 0.0282
	(0,1)	0.0436 \pm 0.00857	0.0180 \pm 0.00388	0.0230 \pm 0.0116
	(1,0)	0.0592 \pm 0.0202	0.0227 \pm 0.00826	0.03002 \pm 0.0267
	(0,0)	0.0622 \pm 0.0322	0.0234 \pm 0.0124	0.0266 \pm 0.0252

Table 4: Experiments on Robustness of loss for continuous treatments. The indicators in the second column denotes whether we use the adversarial training in covariate space (V-GAN) and the reconstruction term for latent features (Z-Rec). Each method was run for five times independently and the standard deviations are shown.

possessed by the original covariates. So we designed experiments to quantitatively evaluate the contribution of the adversarial training in covariate space and the reconstruction in latent space. As shown in Table 4, the reconstruction of latent features could help benefit the model training and achieve slightly better performance. Using the adversarial training in covariate space might not improve the model training as the distribution matching in high-dimensional space might be difficult.

5 Conclusion

In this paper, we developed a novel CausalEGM model, which utilizes the advances in deep generative neural networks for dealing with confounders and estimating the treatment effect in causal inference. CausalEGM enables an efficient encoding, which maps high-dimensional covariates to a low-dimensional latent space. We use GAN-based adversarial training and autoencoder-based reconstruction to guarantee that the latent features are independent of each other and contain the necessary variations in covariates for a good reconstruction.

CausalEGM is flexible to estimate the treatment effect for both individuals and populations under either binary or continuous treatment settings. In a series of systematic experiments, CausalEGM demonstrates superior performance over other existing methods.

A number of extensions and refinements of the CausalEGM model are left open. Here, we provide several directions for further exploration. First, although we use GAN-based adversarial training to guarantee the independence in latent features, it is worth trying to incorporate the approximation error in the generation process to analyze the behavior of CausalEGM’s convergence. Second, the distribution of latent features is set to be a multivariate Gaussian distribution. It is also desirable to make the distribution of latent space more flexible and consider a more general distribution of the latent space, as done by an energy-based model Kohavi and Longbotham (2017). Third, it should be promising to study the complexity of the hyperparameter in CausalEGM when applying to datasets with various sample sizes.

A Proofs of Theorems and Lemmas

Proof of Lemma 2.1

$$\begin{aligned}
\mu(x) &= \int \mathbb{E}(f(x, v, \epsilon) | V = v) p_V(v) dv \\
&= \int \mathbb{E}(f(x, v, \epsilon) | X = x, V = v) p_V(v) dv \quad (\text{by independence of the } \epsilon \text{ and } X \text{ given } V) \\
&= \int \mathbb{E}(Y | X = x, V = v) p_V(v) dv
\end{aligned}$$

Proof of Lemma 3.1 Using the triangle inequality, we have

$$\left\{
\begin{aligned}
\mathbb{E}_0\|Y - \hat{f}_M(X, Z_0, Z_1)\|_2^2 &\leq \mathbb{E}_n\|Y - \hat{f}_M(X, Z_0, Z_1)\|_2^2 + (\mathbb{E}_n - \mathbb{E}_0)(\|Y - \hat{f}_M(X, Z_0, Z_1)\|_2^2) \\
&\leq \mathbb{E}_n\|Y - \hat{f}_M(X, Z_0, Z_1)\|_2^2 + \sup_{f \in \mathcal{F}_M} |(\mathbb{E}_n - \mathbb{E}_0)(\|Y - f(X, Z_0, Z_1)\|_2^2)| \\
\mathbb{E}_0\|X - \hat{h}_M(Z_0, Z_2)\|_2^2 &\leq \mathbb{E}_n\|X - \hat{h}_M(Z_0, Z_2)\|_2^2 + (\mathbb{E}_n - \mathbb{E}_0)(\|X - \hat{h}_M(Z_0, Z_2)\|_2^2) \\
&\leq \mathbb{E}_n\|X - \hat{h}_M(Z_0, Z_2)\|_2^2 + \sup_{h \in \mathcal{F}_M} |(\mathbb{E}_n - \mathbb{E}_0)(\|X - h(Z_0, Z_2)\|_2^2)| \\
\mathbb{E}_0\|V - \hat{g}_M(\hat{e}_M(V))\|_2^2 &\leq \mathbb{E}_n\|V - \hat{g}_M(\hat{e}_M(V))\|_2^2 + (\mathbb{E}_n - \mathbb{E}_0)(\|V - \hat{g}_M(\hat{e}_M(V))\|_2^2) \\
&\leq \mathbb{E}_n\|V - \hat{g}_M(\hat{e}_M(V))\|_2^2 + \sup_{g, e \in \mathcal{F}_M} |(\mathbb{E}_n - \mathbb{E}_0)(\|V - g(e(V))\|_2^2)| \\
d(P_{Z^0}, P_{\hat{e}_M(V)}; \mathcal{A}_M) &\leq d(P_{\hat{e}_M(V)}, P_{Z_{emp}}; \mathcal{A}_M) + d(P_{Z_{emp}}, P_{Z^0}; \mathcal{A}_M)
\end{aligned}
\right. \tag{15}$$

Then by definition of empirical risk minimizer, we further have

$$\left\{
\begin{aligned}
\mathbb{E}_n\|Y - \hat{f}_M(X, Z_0, Z_1)\|_2^2 &\leq \mathbb{E}_n\|Y - f_M^0(X, Z_0, Z_1)\|_2^2 \\
\mathbb{E}_n\|X - \hat{h}_M(Z_0, Z_2)\|_2^2 &\leq \mathbb{E}_n\|X - h_M^0(Z_0, Z_2)\|_2^2 \\
\mathbb{E}_n\|V - \hat{g}_M(\hat{e}_M(V))\|_2^2 &\leq \mathbb{E}_n\|V - g_M^0(e_M^0(V))\|_2^2 \\
d(P_{\hat{e}_M(V)}, P_{Z_{emp}}; \mathcal{A}_M) &\leq d(P_{e_M^0(V)}, P_{Z_{emp}}; \mathcal{A}_M)
\end{aligned}
\right. \tag{16}$$

Then using the triangle inequality again, we have

$$\left\{
\begin{aligned}
\mathbb{E}_n \|Y - f_M^0(X, Z_0, Z_1)\|_2^2 &\leq \mathbb{E}_0 \|Y - f_M^0(X, Z_0, Z_1)\|_2^2 + |(\mathbb{E}_n - \mathbb{E}_0)(\|Y - f_M^0(X, Z_0, Z_1)\|_2^2)| \\
&\leq \mathbb{E}_0 \|Y - f_M^0(X, Z_0, Z_1)\|_2^2 + \sup_{f \in \mathcal{F}_M} |(\mathbb{E}_n - \mathbb{E}_0)(\|Y - f(X, Z_0, Z_1)\|_2^2)| \\
\mathbb{E}_n \|X - h_M^0(Z_0, Z_2)\|_2^2 &\leq \mathbb{E}_0 \|X - h_M^0(Z_0, Z_2)\|_2^2 + |(\mathbb{E}_n - \mathbb{E}_0)(\|X - h_M^0(Z_0, Z_2)\|_2^2)| \\
&\leq \mathbb{E}_0 \|X - h_M^0(Z_0, Z_2)\|_2^2 + \sup_{h \in \mathcal{F}_M} |(\mathbb{E}_n - \mathbb{E}_0)(\|X - h(Z_0, Z_2)\|_2^2)| \\
\mathbb{E}_n \|V - g_M^0(e_M^0(V))\|_2^2 &\leq \mathbb{E}_0 \|V - g_M^0(e_M^0(V))\|_2^2 + |(\mathbb{E}_n - \mathbb{E}_0)(\|V - g_M^0(e_M^0(V))\|_2^2)| \\
&\leq \mathbb{E}_0 \|V - g_M^0(e_M^0(V))\|_2^2 + \sup_{g, e \in \mathcal{F}_M} |(\mathbb{E}_n - \mathbb{E}_0)(\|V - g(e(V))\|_2^2)| \\
d(P_{e_M^0(V)}, P_{Z_{emp}}; \mathcal{A}_M) &\leq d(P_{e_M^0(V)}, P_{Z^0}; \mathcal{A}_M) + d(P_{Z_{emp}}, P_{Z^0}; \mathcal{A}_M)
\end{aligned}
\right. \tag{17}$$

Combine all terms above, we can then get the results.

Proof of theorem 3.2 Each of $\alpha_{M,n}, \beta_{M,n}, \gamma_{M,n}$ and $\zeta_{M,n}$ can be upper bounded by

$$\sup_{F \in \mathcal{F}_M} |(\mathbb{E}_n - \mathbb{E}_0)F| = \sup_{F \in \mathcal{F}_M} \left| \frac{1}{n} \sum_{i=1}^n F(O_i) - \mathbb{E}_0[F(O)] \right|$$

. This is obvious for $\alpha_{M,n}, \beta_{M,n}$, and $\zeta_{M,n}$. To see this for $\gamma_{M,n}$, note if D is the classifier for two measures P_1 and P_2 , and X_i are the observed samples, we then have

$$d(P_1, P_2; \mathcal{A}_M) = \frac{1}{n} \sum_{i=1}^n I_{\{D(X_i)=1\}} - \mathbb{E}_0[I_{\{D(X_i)=1\}}].$$

Now the uniform law of large numbers gives us:

$$\sup_{f \in \mathcal{F}_M} |(\mathbb{E}_n - \mathbb{E}_0)f| \leq 2\mathcal{R}_n(\mathcal{F}_M) + \delta$$

with probability at least $1 - e^{\frac{n\delta^2}{2b^2}}$. We then complete the proof by applying this bound to the combined terms of $\alpha_{m,n}, \beta_{m,n}, \gamma_{m,n}$ and $\zeta_{m,n}$.

Proof of theorem 3.3 Note

$$R_{emp}(f, h, e, g) \stackrel{\Delta}{\leq} R^0(f, h, e, g) + \hat{\alpha}_n + \hat{\beta}_n + \hat{\gamma}_n + \hat{\zeta}_n$$

where

$$\left\{ \begin{array}{l} \hat{\alpha}_n = |(\mathbb{E}_n - \mathbb{E}_0)(\|Y - f(X, Z_0, Z_1)\|_2^2)| \\ \hat{\beta}_n = |(\mathbb{E}_n - \mathbb{E}_0)(\|X - h(Z_0, Z_2)\|_2^2)| \\ \hat{\gamma}_n = d(P_{Z_{emp}}, P_{Z^0}; \mathcal{B}) \\ \hat{\zeta}_n = |(\mathbb{E}_n - \mathbb{E}_0)(\|V - g(e(V))\|_2^2)| \end{array} \right. \quad (18)$$

Then the result is obtained by applying the uniform law of large number in a similar way as the proof of Theorem 3.2.

Proof of theorem 3.4 By Theorem 3.2 for all $\delta' > 0$, we would have

$$(\dagger) : R^0(f^*, h^*, e^*, g^*) \leq R^0(f, h, e, g) + \delta'$$

a.s. for any (f, h, e, g) that can be approximated by neural networks. In particular, we can choose δ' to be the same δ as in Assumption 5. Using the Equations (5) we have for any (f, h, e, g) ,

$$\begin{aligned} R^0(f, h, e, g) &= \mathbb{E}_0\|(f^0 - f)(X, Z_0, Z_1)\|_2^2 + \sigma_1^2 + \mathbb{E}_0\|(h^0 - h)(Z_0, Z_2)\|_2^2 + \sigma_2^2 \\ &\quad + d(P_{Z^0}, P_{e(V)}; \mathcal{A}_M) + \mathbb{E}_0\|(V - d(e(V)))\|_2^2 \end{aligned}$$

Now suppose

$$e'_3, d' = \underset{e_3, d}{\operatorname{argmin}} \{d(P_{Z^0}, P_{(e_0^0, e_1^0, e_2^0, e_3^0)(V)}; \mathcal{A}_M) + \mathbb{E}_0\|V - d((e_0^0, e_1^0, e_2^0, e_3^0)(V))\|_2^2\}$$

Substituting

$$f = f^0, h = h^0, e = (e_0, e_1^0, e_2^0, e_3^0) \text{ and } d = d'$$

into the right-hand side of (†) gives:

$$\begin{aligned}
R^0(f^*, h^*, e^*, g^*) &\leq \sigma_1^2 + \sigma_2^2 + d(P_{Z^0}, P_{(e_0^0, e_1^0, e_2^0, e_3^0)(V)}; \mathcal{A}_M) + \mathbb{E}_0 \|V - d'((e_0^0, e_1^0, e_2^0, e_3^0)(V))\|_2^2 + \delta \\
&\leq \sigma_1^2 + \sigma_2^2 + d(P_{Z^0}, P_{(e_0^0, e_1^0, e_2^0, \tilde{e}_3)(V)}; \mathcal{A}_M) + \mathbb{E}_0 \|V - \tilde{d}((e_0^0, e_1^0, e_2^0, \tilde{e}_3)(V))\|_2^2 + \delta \\
&\stackrel{Asm. 5}{\leq} \sigma_1^2 + \sigma_2^2 + \mathbb{E}_0 \|V - d^*(e^*(V))\|_2^2 + 2\delta
\end{aligned}$$

On the other hand, we have

$$\begin{aligned}
R^0(f^*, h^*, e^*, g^*) &= \mathbb{E}_0 \|(f^0 - f^*)(X, Z_0, Z_1)\|_2^2 + \sigma_1^2 + \mathbb{E}_0 \|(h^0 - h^*)(Z_0, Z_2)\|_2^2 + \sigma_2^2 + \\
&\quad d(P_{Z^0}, P_{e^*(V)}; \mathcal{A}_M) + \mathbb{E}_0 \|(V - d^*)(e^*(V))\|_2^2
\end{aligned} \tag{19}$$

combining with above, we then get the desired inequality.

B Simulation example for Assumption 5

To verify the rationality of Assumption 5 for the consistency analysis, the following simulation study is conducted. Let $V \in \mathcal{V}$ be a continuous random variable that follows a multivariate Gaussian distribution $V \sim N(\boldsymbol{\mu}, \boldsymbol{\Sigma})$ where $\boldsymbol{\mu} \in \mathbb{R}^p$ and $\boldsymbol{\Sigma} \in \mathbb{R}^{p \times p}$. We aim to find encoding function e and generative/decoder function g , which follow the mappings $e : \mathcal{V} \rightarrow \mathbb{R}^q$ and $g : \mathbb{R}^q \rightarrow \mathcal{V}$ where $p < q$. As the covariance matrix $\boldsymbol{\Sigma}$ is symmetric, we can apply the Spectral Theorem. In particular, there is an orthonormal matrix \mathbf{U} and a diagonal matrix $\boldsymbol{\Lambda}$ so that

$$\boldsymbol{\Sigma} = \mathbf{U} \boldsymbol{\Lambda} \mathbf{U}^T \tag{20}$$

where the columns of \mathbf{U} form the eigenvectors associated with the diagonal elements of $\boldsymbol{\Lambda}$. We further sort all the eigenvalues in descending order as $\boldsymbol{\Lambda} = diag(\lambda_1, \dots, \lambda_p)$ where $\lambda_i \geq \lambda_j$ for any $i < j$.

By linear transformation, it is easily proven that $\mathbf{T} = (\mathbf{U}\boldsymbol{\Lambda}^{\frac{1}{2}})^{-1}(\mathbf{V} - \boldsymbol{\mu})$ follows a standard multivariate Gaussian distribution where $\mathbf{T} \sim N(\mathbf{0}, \mathbf{I})$. This linear transformation could be considered as the underlying encoding function where a standard Gaussian distribution is presence in the latent space. In the dimension reduction scenario, it is expected that a small fraction of eigenvalues in $\boldsymbol{\Sigma}$ could explain the majority of the total variation in V . So we design the following generating process.

We set $p = 50$, $q = 13$, and the diagonal elements of $\boldsymbol{\Lambda}$ to be

$$\lambda_i = \begin{cases} 5 - \frac{1}{9}(i-1), & i \leq 10, \\ 0.1 - \frac{1}{400}(i-14), & 14 \leq i \leq 50 \end{cases} \quad (21)$$

where the first 13 principle components can explain 95.96% of the variation contained in V . To generate V , the mean vector $\boldsymbol{\mu}$ is sampled from a uniform distribution $\mu_i \sim U(-1, 1)$, the covariance matrix $\boldsymbol{\Sigma}$ is constructed by Equation (20) where the columns of \mathbf{U} are a set of random orthonormal basis. To construct the features from V for predicting treatment X and outcome Y , we manually set the three components $e_0^0(V)$, $e_1^0(V)$, and $e_2^0(V)$ in the encoder network e as follows

$$\begin{cases} e_0^0(V) = (t_8(V) + t_{11}(V))/\sqrt{2} \\ e_1^0(V) = (t_9(V) + \sum_{i=12}^{20} t_i(V))/\sqrt{10} \\ e_2^0(V) = (t_{10}(V) + \sum_{i=22}^{30} t_i(V))/\sqrt{10} \end{cases} \quad (22)$$

where $t_i(V)$ denotes that i^{th} element of the linear transformation $\mathbf{T} = (\mathbf{U}\boldsymbol{\Lambda}^{\frac{1}{2}})^{-1}(\mathbf{V} - \boldsymbol{\mu})$. It is easily proven that $e_k^0(V) \sim N(0, 1)$ for $k \in \{1, 2, 3\}$, which satisfies the condition 6. The

treatment and outcome can then be generated based on the features of V as

$$\begin{cases} Y = f(X, e_0^0(V), e_1^0(V)) + \epsilon_1 \\ X = h(e_0^0(V), e_2^0(V)) + \epsilon_2 \end{cases} \quad (23)$$

where $e_0^0(V)$, $e_1^0(V)$, and $e_2^0(V)$ can be considered as the constructed features from V for predicting X and Y . For implementation, we set the first three parts of encoder e network to be the fixed functions, $e_0^0(\cdot)$, $e_1^0(\cdot)$, and $e_2^0(\cdot)$. The fourth part of encoder e is trainable, which is set to be 10-dimensional. According to the Principal Component Analysis (PCA) Pearson (1901), the theoretical reconstruction error can be represented as

$$\mathcal{L}_{rec} = \sum_{i=q+1}^p \lambda_i \quad (24)$$

In the above simulation example, $\mathcal{L}_{rec} = 1.907$. Then we generate $N = 50000$ *i.i.d* samples of V . To avoid overfitting of neural nets, we additionally generate 10000 hold-out samples of V . As shown in Figure 3, the empirical reconstruction error of the held-out data reaches the minimum (2.339) at iteration 109600. At such a stopping iteration, the empirical reconstruction error of the training data can be as low as 2.230. In this simulation, δ in assumption 5 can be as small as 0.323, which only occupies 0.68% of all variation contained in V ($\sum_{i=1}^p \lambda_i$).

References

Athey, S. and G. Imbens (2016). Recursive partitioning for heterogeneous causal effects. *Proceedings of the National Academy of Sciences* 113(27), 7353–7360.

Colangelo, K. and Y.-Y. Lee (2020). Double debiased machine learning nonparametric inference with continuous treatments. *arXiv preprint arXiv:2004.03036*.

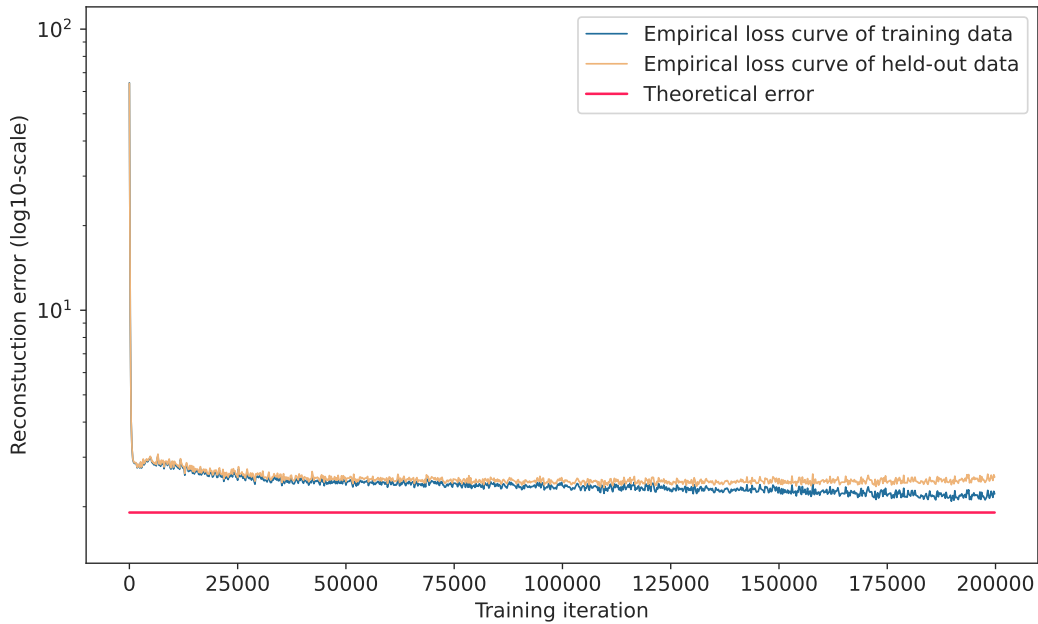


Figure 3: The simulation experiment for verifying the assumption 5

Flores, C. A. et al. (2007). Estimation of dose-response functions and optimal doses with a continuous treatment. *University of Miami, Department of Economics, November*.

Fong, C., C. Hazlett, and K. Imai (2018). Covariate balancing propensity score for a continuous treatment: Application to the efficacy of political advertisements. *The Annals of Applied Statistics* 12(1), 156–177.

Galagat, D. (2016). *Causal inference with a continuous treatment and outcome: Alternative estimators for parametric dose-response functions with applications*. Ph. D. thesis, University of Maryland, College Park.

Gulrajani, I., F. Ahmed, M. Arjovsky, V. Dumoulin, and A. C. Courville (2017). Improved training of wasserstein gans. In I. Guyon, U. V. Luxburg, S. Bengio, H. Wallach, R. Fergus,

S. Vishwanathan, and R. Garnett (Eds.), *Advances in Neural Information Processing Systems*, Volume 30. Curran Associates, Inc.

Guo, S. and M. W. Fraser (2014). *Propensity score analysis: Statistical methods and applications*, Volume 11. SAGE publications.

Hill, J. L. (2011). Bayesian nonparametric modeling for causal inference. *Journal of Computational and Graphical Statistics* 20(1), 217–240.

Hirano, K. and G. W. Imbens (2004). The propensity score with continuous treatments. *Applied Bayesian modeling and causal inference from incomplete-data perspectives* 226164, 73–84.

Imai, K. and D. A. Van Dyk (2004). Causal inference with general treatment regimes: Generalizing the propensity score. *Journal of the American Statistical Association* 99(467), 854–866.

Kennedy, E. H., Z. Ma, M. D. McHugh, and D. S. Small (2017). Non-parametric methods for doubly robust estimation of continuous treatment effects. *Journal of the Royal Statistical Society: Series B (Statistical Methodology)* 79(4), 1229–1245.

Kohavi, R. and R. Longbotham (2017). Online controlled experiments and a/b testing. *Encyclopedia of machine learning and data mining* 7(8), 922–929.

Lee, Y.-Y. (2018). Partial mean processes with generated regressors: Continuous treatment effects and nonseparable models. *arXiv preprint arXiv:1811.00157*.

Li, Y., K. Kuang, B. Li, P. Cui, J. Tao, H. Yang, and F. Wu (2020, 24 Aug). Continuous treatment effect estimation via generative adversarial de-confounding. In *Proceedings of*

the 2020 KDD Workshop on Causal Discovery, Volume 127 of *Proceedings of Machine Learning Research*, pp. 4–22. PMLR.

Liu, Q., J. Xu, R. Jiang, and W. H. Wong (2021). Density estimation using deep generative neural networks. *Proceedings of the National Academy of Sciences* 118(15).

Louizos, C., U. Shalit, J. M. Mooij, D. Sontag, R. Zemel, and M. Welling (2017). Causal effect inference with deep latent-variable models. *Advances in neural information processing systems* 30.

Moodie, E. E. and D. A. Stephens (2012). Estimation of dose–response functions for longitudinal data using the generalised propensity score. *Statistical methods in medical research* 21(2), 149–166.

Panizza, U. and A. F. Presbitero (2014). Public debt and economic growth: is there a causal effect? *Journal of Macroeconomics* 41, 21–41.

Pearson, K. (1901). Liii. on lines and planes of closest fit to systems of points in space. *The London, Edinburgh, and Dublin philosophical magazine and journal of science* 2(11), 559–572.

Robins, J. M. and A. Rotnitzky (2001). Comment on “inference for semiparametric models: Some questions and an answer,” by pj bickel and j. kwon. *Statistica Sinica* 11, 920–936.

Robins, J. M., A. Rotnitzky, and L. P. Zhao (1994). Estimation of regression coefficients when some regressors are not always observed. *Journal of the American statistical Association* 89(427), 846–866.

Rosenbaum, P. R. (1987). Model-based direct adjustment. *Journal of the American statistical Association* 82(398), 387–394.

Rubin, D. B. (1974). Estimating causal effects of treatments in randomized and nonrandomized studies. *Journal of educational Psychology* 66(5), 688.

Schafer, J. and D. Galagate (2015). Causal inference with a continuous treatment and outcome: alternative estimators for parametric dose-response models. *Manuscript in preparation.*

Shalit, U., F. D. Johansson, and D. Sontag (2017). Estimating individual treatment effect: generalization bounds and algorithms. In *International Conference on Machine Learning*, pp. 3076–3085. PMLR.

Shi, C., D. Blei, and V. Veitch (2019). Adapting neural networks for the estimation of treatment effects. *Advances in neural information processing systems* 32.

Stuart, E. A. (2010). Matching methods for causal inference: A review and a look forward. *Statistical science: a review journal of the Institute of Mathematical Statistics* 25(1), 1.

Sun, W., P. Wang, D. Yin, J. Yang, and Y. Chang (2015). Causal inference via sparse additive models with application to online advertising. In *Twenty-Ninth AAAI Conference on Artificial Intelligence*.

Wager, S. and S. Athey (2018). Estimation and inference of heterogeneous treatment effects using random forests. *Journal of the American Statistical Association* 113(523), 1228–1242.

Yoon, J., J. Jordon, and M. Van Der Schaar (2018). Ganite: Estimation of individualized

treatment effects using generative adversarial nets. In *International Conference on Learning Representations*.

Zhang, W., T. D. Le, L. Liu, Z.-H. Zhou, and J. Li (2017). Mining heterogeneous causal effects for personalized cancer treatment. *Bioinformatics* 33(15), 2372–2378.